

# Spatial fluctuations of spin and orbital nature in the two-orbital Hubbard model

Tomoko Kita,<sup>1</sup> Takuma Ohashi,<sup>2</sup> and Sei-ichiro Suga<sup>1</sup>

<sup>1</sup>*Department of Applied Physics, Osaka University, Suita, Osaka 565-0871, Japan*

<sup>2</sup>*Department of Physics, Osaka University, Toyonaka, Osaka 560-0043, Japan*

(Received 19 December 2008; revised manuscript received 23 May 2009; published 24 June 2009)

We investigate the quasiparticle dynamics in the two-orbital Hubbard model on the square lattice at quarter filling by means of the cellular dynamical mean-field theory. We show that the Fermi-liquid state is stabilized up to the large Hubbard interactions in the symmetric case without Hund's coupling, and find the heavy quasiparticles around the metal-insulator boundary. It is elucidated that Hund's coupling enhances the antiferro-orbital correlations, which give rise to the pseudogap behavior in the single-particle excitations. We also find the nonmonotonic temperature dependence in the quasiparticle dynamics for intermediate strength of Hund's coupling, and clarify that it is caused by the competition between the Fermi-liquid formation and the antiferro-orbital fluctuations.

DOI: 10.1103/PhysRevB.79.245128

PACS number(s): 71.30.+h, 71.10.Fd, 71.27.+a

## I. INTRODUCTION

Strongly correlated electron systems with orbital degrees of freedom have attracted much attention. Typical examples are the manganite  $\text{La}_{1-x}\text{Sr}_x\text{MnO}_3$ ,<sup>1</sup> the ruthenate  $\text{Sr}_2\text{RuO}_4$ ,<sup>2</sup> and the vanadate  $\text{LiV}_2\text{O}_4$ ,<sup>3</sup> where striking phenomena such as colossal magnetoresistance, triplet superconductivity, and heavy fermion behavior have been observed. The importance of orbital degrees of freedom has been suggested also in unconventional superconductors such as  $\text{Na}_x\text{CoO}_2\cdot y\text{H}_2\text{O}$  (Ref. 4) and the newly discovered iron-based superconductor  $\text{LaFeAsO}_{1-x}\text{F}_x$ .<sup>5</sup>

These interesting experimental findings have stimulated a number of theoretical works on electron correlations in the multiorbital systems. Among them, the dynamical mean-field theory (DMFT) (Ref. 6) has successfully applied to the multiorbital systems.<sup>7-17</sup> The long standing issue of itinerant ferromagnetism has been investigated by DMFT,<sup>9,17</sup> and it has been clarified that not only the lattice structure but also orbital fluctuations under strong influence of Hund's coupling is important for the realization of ferromagnetism. The Mott transition in the multiorbital systems has been also studied extensively by means of DMFT. One of important conclusions of DMFT is that orbital degeneracy strongly enhances fluctuations of spin, charge, and orbital, which stabilize the renormalized metallic state.<sup>12</sup> The observation of the orbital-selective Mott transition in  $\text{Ca}_{2-x}\text{Sr}_x\text{RuO}_4$  (Ref. 18) has further stimulated studies on the metal-insulator transition in the multiorbital systems. The DMFT studies on the two-orbital Hubbard model with different bandwidths have clarified that orbital fluctuations play a key role in the orbital-selective Mott transition.<sup>11-14</sup> However, the effects of the spatial correlations on the Mott transition in the multiorbital systems have not yet been well understood because the DMFT does not treat spatially extended correlations. Therefore, it is desirable to investigate how the spatial fluctuations of spin and orbital affect quasiparticle dynamics around the Mott transition in the multiorbital system, using a different appropriate method.

In this paper, we study the effects of spatial fluctuations of spin and orbital on the quasiparticle dynamics in the two-

orbital Hubbard model at quarter filling, using the cellular dynamical mean-field theory (CDMFT) (Ref. 19) combined with the noncrossing approximation (NCA).<sup>20,21</sup> In the absence of Hund's coupling, we show that the metallic state persists up to large Coulomb interactions. This gives rise to the heavy quasiparticle behavior around the metal-insulator boundary. It is clarified that Hund's coupling strongly enhances the antiferro-orbital (AFO) fluctuations, which suppress the quasiparticle formation. Strong Hund's coupling induces the pseudogap in the single-particle spectra. In the intermediate regime of Hund's coupling, we find more striking behavior, namely, a unique nonmonotonic temperature dependence of the single-particle excitations: the heavy quasiparticles once develop with lowering temperatures, and then they are suppressed at much lower temperatures. It is elucidated that this nonmonotonic temperature dependence of the single-particle excitations is caused by the competition between the quasiparticle formation and the AFO correlations.

## II. MODEL AND METHOD

We consider the two-orbital Hubbard model on the two-dimensional square lattice,

$$H = -t \sum_{\langle i,j \rangle \alpha \sigma} c_{i\alpha\sigma}^\dagger c_{j\alpha\sigma} + U \sum_{i\alpha} n_{i\alpha\uparrow} n_{i\alpha\downarrow} + \sum_{i\sigma\sigma'} (U' - \delta_{\sigma\sigma'} J) n_{i1\sigma} n_{i2\sigma'} - J \sum_i (c_{i1\uparrow}^\dagger c_{i1\downarrow}^\dagger c_{i2\downarrow}^\dagger c_{i2\uparrow} + c_{i1\uparrow}^\dagger c_{i1\downarrow}^\dagger c_{i2\uparrow}^\dagger c_{i2\downarrow} + \text{H.c.}), \quad (1)$$

where  $c_{i\alpha\sigma}^{(\dagger)}$  is an annihilation (creation) operator with spin  $\sigma(=\uparrow, \downarrow)$  and orbital  $\alpha(=1, 2)$  at the  $i$ th site, and  $n_{i\alpha\sigma} = c_{i\alpha\sigma}^\dagger c_{i\alpha\sigma}$  is the number operator. Here,  $t$  denotes the nearest-neighbor hopping integral,  $U(U')$  is the intraorbital (interorbital) Coulomb interaction, and  $J$  is Hund's coupling including the spin-flip and pair-hopping terms. We impose the condition  $U=U'+2J$  due to the symmetry requirement.

In order to investigate the effects of spatially extended spin and orbital fluctuations around the Mott transition, we

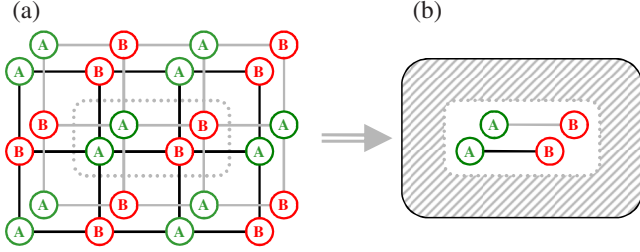


FIG. 1. (Color online) (a) Sketch of the two-orbital Hubbard model on the square lattice and (b) the effective cluster model using two-site/two-orbital cluster CDMFT.

employ CDMFT, a cluster extension of DMFT. In CDMFT, the original lattice is regarded as a superlattice consisting of clusters, which is then mapped onto an effective cluster model via a DMFT-type procedure. We use a two-site cluster model coupled to the self-consistently determined medium. We note that the tiling of the original lattice in two-site clusters is not unique. Here, we define each site in the two-site cluster as the sites  $A$  and  $B$ . In order to incorporate the anti-ferromagnetic (AFM) and AFO correlations, we choose a tiling configuration as shown in Fig. 1, where the site  $A$  is next to the site  $B$ . Using the above method, we can treat the short-range correlations of spin and orbital within the two-site cluster. The effective cluster Hamiltonian is obtained as,

$$\begin{aligned}
 H_{\text{eff}} = & \sum_{ij\alpha\sigma} t_{ij} c_{i\alpha\sigma}^\dagger c_{j\alpha\sigma} - \mu \sum_{i\alpha\sigma} n_{i\alpha\sigma} + U \sum_{i\alpha} n_{i\alpha\uparrow} n_{i\alpha\downarrow} \\
 & + \sum_{i\sigma\sigma'} (U' - \delta_{\sigma\sigma'} J) n_{i1\sigma} n_{i2\sigma'} - J \sum_i (c_{i1\uparrow}^\dagger c_{i1\downarrow}^\dagger c_{i2\downarrow}^\dagger c_{i2\uparrow} \\
 & + c_{i1\uparrow}^\dagger c_{i1\downarrow}^\dagger c_{i2\uparrow} c_{i2\downarrow} + \text{H.c.}) + \sum_k \sum_{\alpha\sigma} \varepsilon_{k\alpha\sigma} a_{k\alpha\sigma}^\dagger a_{k\alpha\sigma} \\
 & + \sum_k \sum_{i\alpha\sigma} (V_{ki\alpha\sigma} a_{k\alpha\sigma}^\dagger c_{i\alpha\sigma} + \text{H.c.}), \quad (2)
 \end{aligned}$$

where  $\mu$  is the chemical potential and  $t_{ij}$  is the hopping matrix elements in the two-site cluster, respectively. Effective bath fermions with the energy  $\varepsilon_{k\alpha\sigma}$  are created by  $a_{k\alpha\sigma}^\dagger$  and coupled to electrons in cluster sites via  $V_{ki\alpha\sigma}$ . Here,  $i$  corresponds to the cluster indices ( $i=A, B$ ),  $\alpha$  is the orbital index ( $\alpha=1, 2$ ),  $\sigma$  is the spin index ( $\sigma=\uparrow, \downarrow$ ), and  $k$  labels infinite bath degrees of freedom. In effective model (2), we calculate the cluster Green's function  $\hat{G}_{\alpha\sigma}$  by means of NCA as,

$$\hat{G}_{\alpha\sigma}(\omega) = [(\omega + \mu)\hat{1} - \hat{t} - \hat{\Gamma}_{\alpha\sigma}(\omega) - \hat{\Sigma}_{\alpha\sigma}(\omega)]^{-1}, \quad (3)$$

where  $\hat{\Sigma}_{\alpha\sigma}$  is the self-energy. Here,  $\hat{O}$  denotes  $2 \times 2$  matrix for fixed  $\alpha$  and  $\sigma$ . The effective medium is described by the hybridization function  $\Gamma_{ij\alpha\sigma}(\omega) = \sum_k V_{ki\alpha\sigma} V_{kj\alpha\sigma}^* (\omega - \varepsilon_{k\alpha\sigma})$ . In terms of the self-energy  $\hat{\Sigma}_{\alpha\sigma}$ , the hybridization function is recomputed by

$$\begin{aligned}
 \hat{\Gamma}_{\alpha\sigma}(\omega) = & (\omega + \mu)\hat{1} - \hat{t} - \hat{\Sigma}_{\alpha\sigma}(\omega) \\
 & - \left[ \frac{1}{N} \sum_{\mathbf{K}} \frac{1}{(\omega + \mu)\hat{1} - \hat{t}(\mathbf{K}) - \hat{\Sigma}_{\alpha\sigma}(\omega)} \right]^{-1}, \quad (4)
 \end{aligned}$$

where the summation of  $\mathbf{K}$  is taken over the reduced Brillouin zone of the superlattice. Here,  $\hat{t}(\mathbf{K})$  is the Fourier-transformed hopping matrix for the superlattice. This procedure is iterated until numerical convergence is reached.

In DMFT or the cluster extensions of DMFT, a solver of effective Hamiltonian (2) is important. The numerically exact solvers are the numerical renormalization group (NRG),<sup>22,23</sup> density-matrix renormalization group (DMRG),<sup>24</sup> and quantum Monte Carlo (QMC) method,<sup>25,26</sup> which are computationally expensive. As an approximate method, the exact diagonalization (ED), iterative perturbation theory (IPT), NCA, etc. have been used.<sup>6</sup> NRG (Refs. 23 and 27) and DMRG (Refs. 28–30) have been successfully applied to single-site DMFT but it is difficult to apply them to cluster DMFT (Ref. 31) or multiorbital systems. In cluster DMFT combined with Hirsch-Fye QMC,<sup>25,31–37</sup> it is known that the sign problem becomes serious due to Hund's coupling or the pair hopping in the multiorbital system.<sup>16,17</sup> In CDMFT+ED,<sup>38–40</sup> the finite-size errors in the effective model [finite  $k$  points in Eq. (2)] become larger in the two-band model than the single-band model due to the memory limitation. IPT, which is the second-order perturbation expansion in  $U$ , gives a good approximation in the single-band Hubbard model or periodic Anderson model in the infinite dimensions<sup>6</sup> but it is qualitatively incorrect for the multi-orbital models or cluster DMFT. On the other hand, in NCA, neither finite-size error nor sign problem arises. It is known that DMFT+NCA works well, not only in the single-band models but also in the multiorbital models.<sup>10</sup> The cluster DMFT combined with the NCA has also been successfully applied to the single-band Hubbard model<sup>21,31,41–43</sup> and  $t$ - $j$  model.<sup>44,45</sup> In CDMFT+NCA, we do not encounter much more serious problems in the two-orbital Hubbard model than in the single-band model. Therefore, we employ NCA as a solver of effective model (2). NCA is a perturbation expansion around the molecular limit and computationally inexpensive. In general, it gives rise to artificial non-Fermi liquid (NFL) properties at lower temperatures than the Fermi liquid (FL) coherence temperature.<sup>20</sup> In the following discussion, we restrict our analysis to the temperature region around and higher than the FL coherence temperature.

### III. RESULTS

Let us now investigate spatial fluctuations of spin and orbital in the two-orbital Hubbard model at quarter filling using CDMFT+NCA. We have confirmed that our results for  $U'=J=0$ , which corresponds to the single-band Hubbard model, are consistent with the previous results.<sup>21</sup> We first study the case without Hund's coupling. In Fig. 2, we show the density of states (DOS) for  $U=U'$ ,  $J=0$  at a temperature  $T/t=0.1$ . Here, the DOS per spin and orbital is defined as  $\rho(\omega) = -\text{Im} G_{ii\alpha\sigma}(\omega + i0)/\pi$ . We can clearly see the metal-insulator crossover in the DOS. As  $U$  increases, the quasipar-

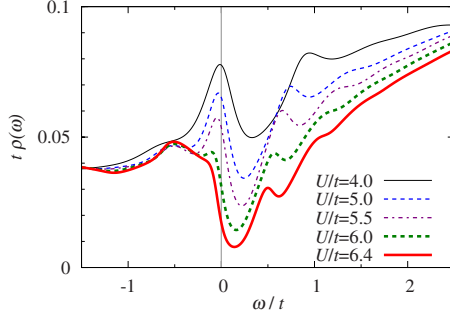


FIG. 2. (Color online) Density of states at  $T/t=0.1$  for several interaction strengths  $U=U'$  without Hund's coupling  $J=0$ .

title peak around the Fermi level becomes sharper. We can clearly see the heavy quasiparticle peak for  $U/t=4.0$  in Fig. 2. As further increasing  $U$ , the quasiparticle peak is suppressed and vanishes at  $U/t \sim 5.8$ . For  $U/t > 5.8$ , a gap is formed near the Fermi level and the system becomes insulating. We thus find that the metal-insulator boundary exists at  $U/t \sim 5.8$  for  $T/t=0.1$ . The  $T$  dependence of the DOS is shown in Fig. 3. In the metallic phase ( $U/t=4.0$ ), the quasiparticle peak appears near the Fermi level, as  $T$  is lowered below the FL coherence temperature  $T_0/t \sim 0.5$ . Here,  $T_0$  is defined as the width of the quasiparticle peak at low temperatures. Around the metal-insulator boundary ( $U/t=5.0$ ), the coherence temperature becomes lower ( $T_0/t \sim 0.3$ ) and the sharper peak develops at low temperatures. This behavior clearly demonstrates the evolution of the heavy quasiparticle at low temperatures. On the other hand, in the insulating phase for  $U/t=6.0$ , the gap becomes more prominent with lowering  $T$  although DOS at the Fermi level  $\rho(0)$  is finite at  $T/t \geq 0.05$ . At much lower temperatures,  $\rho(0)$  should vanish and the system is expected to be a real insulator. These results are quite different from those of the single-band Hubbard model at half filling on the square lattice<sup>21,31,32,41</sup> but are consistent with those of single-site DMFT.<sup>8,14</sup> In the former case, where one electron occupies each site as well as our model, the FL quasiparticle is strongly suppressed by AFM fluctuations. On the other hand, in the latter case, where spatial correlations are not taken into account, the quasiparticle peak appears around the Mott transition. Therefore, in our

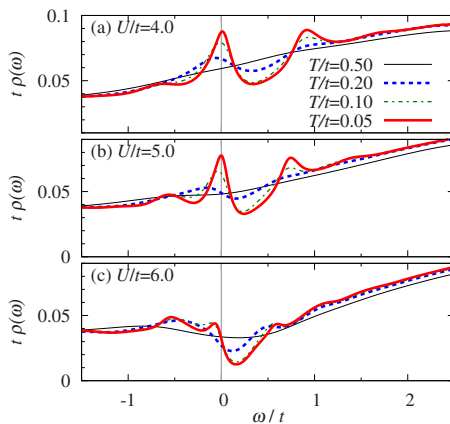


FIG. 3. (Color online) Temperature dependence of the density of states at (a)  $U/t=U'/t=4.0$ , (b) 5.0, and (c) 6.0 for  $J=0$ .

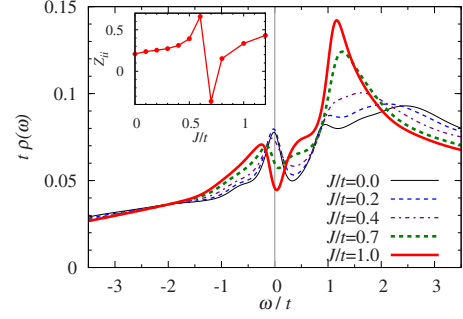


FIG. 4. (Color online) Density of states for  $U/t=4.0$  at  $T/t=0.1$  with varying  $J$ . The inset shows the renormalization factor as a function of  $J$ . The renormalization factor for  $J/t > 0.7$  has no meaning because of the Fermi-liquid breakdown.

case, spatial correlations of spin and orbital are strongly suppressed by orbital degeneracy, and the FL quasiparticles are stabilized.

We next investigate the system with Hund's coupling. In the presence of Hund's coupling, we find that the spatial correlations give rise to the pseudogap in the quasiparticle excitation. In Fig. 4, we show the DOS for  $U/t=4.0$  at  $T/t=0.1$  with varying Hund's coupling  $J$ . As Hund's coupling  $J$  increases, the quasiparticle peak gradually shrinks and vanishes for  $J/t \sim 0.7$ . As  $J$  further increases, a pseudogap evolves and the system becomes insulating. We note that this behavior caused by Hund's coupling  $J$  is qualitatively different from the results of single-site DMFT.<sup>14</sup> Within DMFT, which does not treat the spatial correlations, it is known that Hund's coupling reduces the energy gap of the Mott insulator to  $U' - J$ . Therefore, in DMFT, Hund's coupling reduces the effective Coulomb repulsion and tends to stabilize the metallic phase. The previous DMFT+NCA studies show that the quasiparticle peak in DOS get enhanced as  $J$  increases.<sup>10</sup> On the other hand, in our CDMFT, which properly incorporate spatial correlations, Hund's coupling enhances spatial correlations of spin and orbital, which give rise to the NFL state with the pseudogap.

The NFL behavior is also seen in the renormalization factor  $\hat{Z} = [\hat{1} - \partial \text{Re } \hat{\Sigma}(\omega + i0) / \partial \omega|_{\omega=0}]^{-1}$ . In the inset of Fig. 4, we show  $Z_{ii}$  as a function of  $J$ . With increasing  $J$ , the renormalization factor  $Z_{ii}$  increases and jumps to negative values at  $J/t \sim 0.7$ . The negative values of  $Z_{ii}$  indicate the breakdown of FL. We thus find the crossover from FL to NFL states at  $J/t \sim 0.7$ . This behavior is consistent with the results of DOS in Fig. 4. In single-site DMFT, the renormalization factor increases as  $J$  increases but its mechanism is completely different from that in our case. Within DMFT, the effective interaction is reduced by  $J$ , as mentioned above.<sup>14</sup> Therefore, the renormalization factor increases and the FL metallic state is stabilized. On the other hand, in our CDMFT, which incorporates not only such local renormalization effects of  $J$  but also nonlocal correlations,  $Z_{ii}$  increases and shows the NFL properties. This behavior is also seen in the dynamical cluster studies of the single-band Hubbard model at half filling.<sup>31,41</sup> In this case, the AFM correlations disturb the FL formation and induce the NFL behavior. In our case, the AFO correlations enhanced by Hund's coupling trigger the NFL properties in  $Z_{ii}$ .

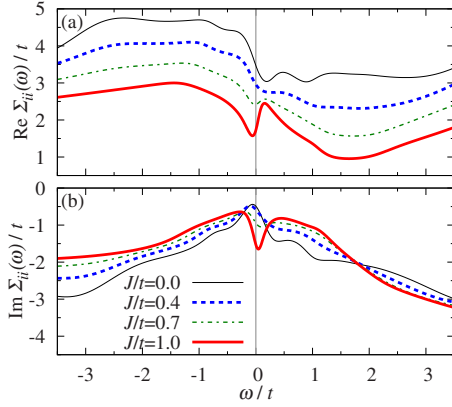


FIG. 5. (Color online) (a) The real part and (b) the imaginary part of the self-energy for  $U/t=4.0$  at  $T/t=0.1$  with varying  $J$ .

In Fig. 5, we also show the local self-energy  $\Sigma_{ii}(\omega+i0)$  for typical values of  $J$ . For small  $J$  ( $J/t=0, 0.4$ ),  $\text{Im } \Sigma_{ii}(\omega+i0)$  is small and  $\partial \text{Re } \Sigma_{ii}(\omega+i0)/\partial \omega$  is negative at  $\omega=0$ , which is FL-like behavior. As  $J$  increases,  $\text{Im } \Sigma_{ii}(\omega+i0)$  at  $\omega=0$  increases in the negative direction and the profile of  $\text{Im } \Sigma_{ii}(\omega+i0)$  dramatically changes in the large  $J$  region ( $J/t=1.0$ ). Also,  $\partial \text{Re } \Sigma_{ii}(\omega+i0)/\partial \omega$  at  $\omega=0$  changes its sign from negative to positive at  $J/t \sim 0.7$ . These results are consistent with the results of DOS and the renormalization factor.

To clarify how the insulating state is induced by spatial correlations, we calculate the nearest-neighbor spin-correlation function  $\langle S_i^z S_{i+1}^z \rangle$  and orbital correlation function  $\langle \tau_i^z \tau_{i+1}^z \rangle$ . Here,  $S_i^z$  and  $\tau_i^z$  are defined as  $S_i^z = \sum_{\alpha} (n_{i\alpha\uparrow} - n_{i\alpha\downarrow})/2$  and  $\tau_i^z = \sum_{\sigma} (n_{i1\sigma} - n_{i2\sigma})/2$ , respectively. In Fig. 6(a), we show the  $T$  dependence of the spin-correlation function  $\langle S_i^z S_{i+1}^z \rangle$  for several values of  $J$ . For  $J=0$ ,  $\langle S_i^z S_{i+1}^z \rangle$  is always negative so that the spin correlations are AFM, which are monotonically enhanced with lowering  $T$ . On the other hand, for the finite Hund's coupling  $J$ ,  $\langle S_i^z S_{i+1}^z \rangle$  once decreases as  $T$  decreases and then upturns, taking a minimum at  $T=T^*$ . At much lower temperatures,  $\langle S_i^z S_{i+1}^z \rangle$  tends to become positive and the spin correlations are expected to be ferromagnetic (FM). For the larger interaction  $U/t=6.0$ , we find that the spin FM correlations are more enhanced at low temperatures. This behavior indicates that the effects of Hund's coupling become prominent at  $T < T^*$ , and the AFM correlations are strongly

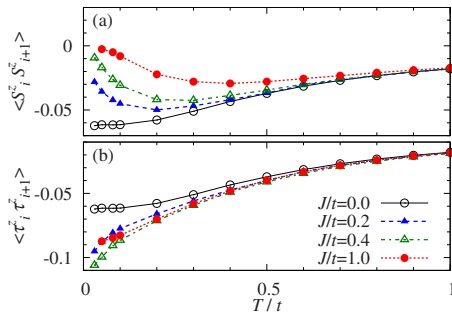


FIG. 6. (Color online) Nearest-neighbor correlation functions of (a) spin  $\langle S_i^z S_{i+1}^z \rangle$  and (b) orbital  $\langle \tau_i^z \tau_{i+1}^z \rangle$ , as a function of the temperature  $T$  at  $U/t=4.0$ .

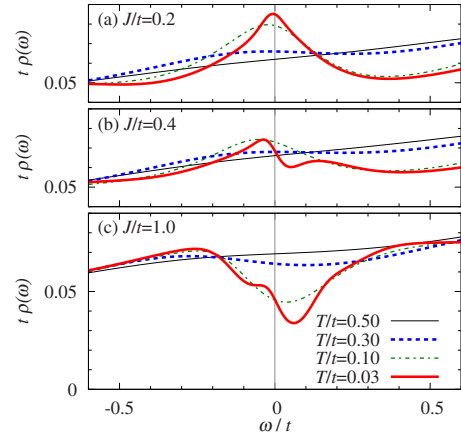


FIG. 7. (Color online) Temperature dependence of the density of states at  $U/t=4.0$  for (a)  $J/t=0.2$ , (b)  $J/t=0.4$ , and (c)  $J/t=1.0$ .

suppressed. The characteristic temperature  $T^*$  increases with increasing  $J$ :  $T^*/t \sim 0.2, 0.3$ , and  $0.4$  for  $J/t=0.2, 0.4$ , and  $1.0$ , respectively. Figure 6(b) shows the  $T$  dependence of the orbital correlation function  $\langle \tau_i^z \tau_{i+1}^z \rangle$ . The orbital correlation functions are negative and the correlations are AFO. As  $T$  decreases, the AFO correlations gradually become strong and get strongly enhanced at  $T < T^*$  in the presence of Hund's coupling. For  $J/t=1.0$ , the AFO correlations are suppressed at low temperatures, which is due to the suppression of the orbital moment by Hund's coupling.

The noticeable point is that the AFO correlations for  $J=0$  at low temperatures are much weaker than those for finite  $J$ . For  $U=U'$ , spin and orbital states in two adjacent sites are highly degenerate, i.e., AFM and AFO, AFM and ferro-orbital, and FM and AFO states are all degenerate because of the spin and orbital symmetries. This degeneracy strongly suppresses the nearest-neighbor spin and orbital correlations. On the other hand, Hund's coupling lifts the degeneracy, and strongly enhances the AFO fluctuations at  $T < T^*$ . These spatial correlations also affect the quasiparticle dynamics. For  $J=0$ , where the correlations are very weak due to the degeneracy, the FL state is stabilized and the heavy quasiparticle peak instead of the pseudogap appears in the DOS, as seen in Fig. 3. On the other hand, the AFO correlations get strongly enhanced under influence of Hund's coupling, and these correlations induce the pseudogap behavior in the DOS, as shown in Fig. 4.

By investigating the  $T$  dependence of the DOS for the different  $J$ , we find more striking behavior in the quasiparticle dynamics. In Fig. 7, we show the  $T$  dependence of the DOS for  $U/t=4.0$  with varying Hund's coupling  $J/t=0.2, 0.4$ , and  $1.0$ . For the weak Hund's coupling  $J/t=0.2$ , the quasiparticle peak appears at  $T < T_0$ , which becomes sharper with lowering  $T$  as well as the case without Hund's coupling shown in Fig. 3. In contrast, for the strong Hund's coupling  $J/t=1.0$ , the pseudogap appears around the Fermi level, and the gap becomes prominent at  $T < T^* \sim 0.4t$ . For intermediate Hund's coupling  $J/t=0.4$ , the two energy scales,  $T_0$  and  $T^*$ , become relevant to the quasiparticle dynamics. This results in the nonmonotonic  $T$  dependence of the DOS. For  $J/t=0.4$ , as  $T$  decreases, the quasiparticle peak once develops at  $T < T_0$ . At much lower temperatures  $T < T^* \sim 0.3t$ , the AFO



correlations get enhanced, and the DOS shows insulating behavior with a dip near the Fermi level. We thus conclude that the nonmonotonic  $T$  dependence is induced by the competition between the FL formation and the AFO correlations.

#### IV. SUMMARY

We have studied the effects of spatial fluctuations in the two-orbital Hubbard model at quarter filling by means of CDMFT+NCA. We have found the heavy quasiparticle behavior around the metal-insulator boundary, which is caused by orbital degeneracy. It has been clarified that Hund's coupling enhances the AFO fluctuations, which give rise to the pseudogap behavior of the DOS. We have also found a unique nonmonotonic  $T$  dependence in the single-particle excitations<sup>36</sup> caused by the FL formation and the AFO correlations for the intermediate Hund's coupling.

It has been suggested that the ground state of the two-orbital Hubbard model at quarter filling is FM and AFO ordered states in strong coupling region.<sup>9,46</sup> Also in our study, we have found that the AFO correlations get enhanced by spatial fluctuations due to Hund's coupling, which is naturally expected to stabilize the ordered phase at zero temperature. In the two-dimensional  $SU(4)$  spin-orbital model, the importance of the plaquette singlet correlation has been pointed out.<sup>47</sup> In our CDMFT, however, we have used the two-site effective cluster model as a minimal model to study

the effects of the spatial fluctuations and have not incorporate the spin and orbital fluctuations in a plaquette. Therefore, the effects of the correlations in the plaquette should be studied using the larger cluster CDMFT. Also, to quantitatively improve our results, we should use the essentially exact cluster solver such as the continuous-time quantum Monte Carlo method, in our future work. On the other hand, in real materials with the interlayer hopping, the correlations in a plaquette are not strong but the AFO correlations are expected to be dominant. Therefore, we expect that our findings in the present study, such as the heavy FL behavior and the nonmonotonic  $T$  dependence in quasiparticle excitations, will be observed experimentally in the correlated electron systems with orbital degeneracy.

#### ACKNOWLEDGMENTS

The authors thank H. Tsunetsugu, N. Kawakami, T. Momoi, and K. Inaba for valuable discussions. This work has been supported by the Japan Society for the Promotion of Science, Grant-in-Aid for Scientific Research (Grants No. 21740232 and No. 20540390), the Next Generation Supercomputing Project, and Nanoscience Program from the Ministry of Education Science Sports and Culture of Japan. A part of the computations was done at the Supercomputer Center at the Institute for Solid State Physics, University of Tokyo and Yukawa Institute Computer Facility.

- 
- <sup>1</sup>Y. Tokura, A. Urushibara, Y. Moritomo, T. Arima, A. Asamitsu, G. Kido, and N. Furukawa, *J. Phys. Soc. Jpn.* **63**, 3931 (1994).
  - <sup>2</sup>Y. Maeno, H. Hashimoto, K. Tshida, S. Nishizaki, T. Fujita, J. G. Bednorz, and F. Lichtenberg, *Nature (London)* **372**, 532 (1994).
  - <sup>3</sup>S. Kondo, D. C. Johnston, C. A. Swenson, F. Borsa, A. V. Mahajan, L. L. Miller, T. Gu, A. I. Goldman, M. B. Maple, D. A. Gajewski, E. J. Freeman, N. R. Dilley, R. P. Dickey, J. Merrin, K. Kojima, G. M. Luke, Y. J. Uemura, O. Chmaissem, and J. D. Jorgensen, *Phys. Rev. Lett.* **78**, 3729 (1997).
  - <sup>4</sup>K. Takada, H. Sakurai, E. Takayama-Muromachi, F. Izumi, R. A. Dilaian, and T. Sasaki, *Nature (London)* **422**, 53 (2003).
  - <sup>5</sup>Y. Kamihara, T. Watanabe, M. Hirano, and H. Hosono, *J. Am. Chem. Soc.* **130**, 3296 (2008).
  - <sup>6</sup>A. Georges, G. Kotliar, W. Krauth, and M. J. Rozenberg, *Rev. Mod. Phys.* **68**, 13 (1996).
  - <sup>7</sup>G. Kotliar and H. Kajueter, *Phys. Rev. B* **54**, R14221 (1996).
  - <sup>8</sup>M. J. Rozenberg, *Phys. Rev. B* **55**, R4855 (1997).
  - <sup>9</sup>T. Momoi and K. Kubo, *Phys. Rev. B* **58**, R567 (1998).
  - <sup>10</sup>Y. Imai and N. Kawakami, *J. Phys. Soc. Jpn.* **70**, 2365 (2001).
  - <sup>11</sup>A. Koga, N. Kawakami, T. M. Rice, and M. Sigrist, *Phys. Rev. Lett.* **92**, 216402 (2004).
  - <sup>12</sup>A. Koga, K. Inaba, and N. Kawakami, *Prog. Theor. Phys.* **160**, 253 (2005).
  - <sup>13</sup>K. Inaba, A. Koga, S.-I. Suga, and N. Kawakami, *Phys. Rev. B* **72**, 085112 (2005).
  - <sup>14</sup>K. Inaba and A. Koga, *J. Phys. Soc. Jpn.* **76**, 094712 (2007).
  - <sup>15</sup>R. Arita, K. Held, A. V. Lukoyanov, and V. I. Anisimov, *Phys. Rev. Lett.* **98**, 166402 (2007).
  - <sup>16</sup>S. Sakai, R. Arita, K. Held, and H. Aoki, *Phys. Rev. B* **74**, 155102 (2006).
  - <sup>17</sup>S. Sakai, R. Arita, and H. Aoki, *Phys. Rev. Lett.* **99**, 216402 (2007).
  - <sup>18</sup>S. Nakatsuji, D. Hall, L. Balicas, Z. Fisk, K. Sugahara, M. Yoshioka, and Y. Maeno, *Phys. Rev. Lett.* **90**, 137202 (2003).
  - <sup>19</sup>G. Kotliar, S. Y. Savrasov, G. Palsson, and G. Biroli, *Phys. Rev. Lett.* **87**, 186401 (2001).
  - <sup>20</sup>N. E. Bickers, *Rev. Mod. Phys.* **59**, 845 (1987).
  - <sup>21</sup>T. D. Stanescu, M. Civelli, K. Haule, and G. Kotliar, *Ann. Phys.(N.Y.)* **321**, 1682 (2006).
  - <sup>22</sup>K. G. Wilson, *Rev. Mod. Phys.* **47**, 773 (1975).
  - <sup>23</sup>R. Bulla, T. A. Costi, and T. Pruschke, *Rev. Mod. Phys.* **80**, 395 (2008).
  - <sup>24</sup>S. R. White, *Phys. Rev. Lett.* **69**, 2863 (1992).
  - <sup>25</sup>J. E. Hirsch and R. M. Fye, *Phys. Rev. Lett.* **56**, 2521 (1986).
  - <sup>26</sup>P. Werner, A. Comanac, L. de' Medici, M. Troyer, and A. J. Millis, *Phys. Rev. Lett.* **97**, 076405 (2006).
  - <sup>27</sup>R. Bulla, *Phys. Rev. Lett.* **83**, 136 (1999).
  - <sup>28</sup>D. J. García, K. Hallberg, and M. J. Rozenberg, *Phys. Rev. Lett.* **93**, 246403 (2004).
  - <sup>29</sup>S. Nishimoto, F. Gebhard, and E. Jeckelmann, *J. Phys.: Condens. Matter* **16**, 7063 (2004).
  - <sup>30</sup>M. Karski, C. Raas, and G. S. Uhrig, *Phys. Rev. B* **72**, 113110 (2005).
  - <sup>31</sup>T. Maier, M. Jarrell, T. Pruschke, and M. H. Hettler, *Rev. Mod. Phys.* **77**, 1027 (2005).

- <sup>32</sup>S. Moukouri and M. Jarrell, Phys. Rev. Lett. **87**, 167010 (2001).
- <sup>33</sup>O. Parcollet, G. Biroli, and G. Kotliar, Phys. Rev. Lett. **92**, 226402 (2004).
- <sup>34</sup>P. Sun and G. Kotliar, Phys. Rev. Lett. **95**, 016402 (2005).
- <sup>35</sup>T. Ohashi, N. Kawakami, and H. Tsunetsugu, Phys. Rev. Lett. **97**, 066401 (2006).
- <sup>36</sup>T. Ohashi, T. Momoi, H. Tsunetsugu, and N. Kawakami, Phys. Rev. Lett. **100**, 076402 (2008).
- <sup>37</sup>S. Sakai, Y. Motome, and M. Imada, Phys. Rev. Lett. **102**, 056404 (2009).
- <sup>38</sup>M. Civelli, M. Capone, S. S. Kancharla, O. Parcollet, and G. Kotliar, Phys. Rev. Lett. **95**, 106402 (2005).
- <sup>39</sup>B. Kyung and A.-M. S. Tremblay, Phys. Rev. Lett. **97**, 046402 (2006).
- <sup>40</sup>Y. Z. Zhang and M. Imada, Phys. Rev. B **76**, 045108 (2007).
- <sup>41</sup>Y. Imai and N. Kawakami, Phys. Rev. B **65**, 233103 (2002).
- <sup>42</sup>T. Maier, M. Jarrell, T. Pruschke, and J. Keller, Phys. Rev. Lett. **85**, 1524 (2000).
- <sup>43</sup>T. Maier, M. Jarrell, T. Pruschke, and J. Keller, Eur. Phys. J. B **13**, 613 (2000).
- <sup>44</sup>K. Haule and G. Kotliar, Phys. Rev. B **76**, 104509 (2007).
- <sup>45</sup>T. A. Maier, D. Poilblanc, and D. J. Scalapino, Phys. Rev. Lett. **100**, 237001 (2008).
- <sup>46</sup>K. Kubo, Phys. Rev. B **79**, 020407(R) (2009).
- <sup>47</sup>Y. Q. Li, M. Ma, D. N. Shi, and F. C. Zhang, Phys. Rev. Lett. **81**, 3527 (1998).